Light field constancy within natural scenes

Alexander A. Mury,* Sylvia C. Pont, and Jan J. Koenderink

Department of Physics and Astronomy, Physics of Man, Helmholtz Institute, Utrecht University Princetonplein 5, NL 3584 CC Utrecht, The Netherlands

*Corresponding author: a.mury@phys.uu.nl

Received 8 February 2007; accepted 7 May 2007;
posted 17 August 2007 (Doc. ID 79798); published 9 October 2007

The structure of light fields of natural scenes is highly complex due to high frequencies in the radiance distribution function. However it is the low-order properties of light that determine the appearance of common matte materials. We describe the local light field in terms of spherical harmonics and analyze the qualitative properties and physical meaning of the low-order components. We take a first step in the further development of Gershun's classical work on the light field by extending his description beyond the 3D vector field, toward a more complete description of the illumination using tensors. We show that the three first components, namely, the monopole (density of light), the dipole (light vector), and the quadrupole (squash tensor) suffice to describe a wide range of qualitatively different light fields.

In this paper we address a related issue, namely, the spatial properties of light fields within natural scenes. We want to find out to what extent local light fields change from point to point and how different orders behave. We found experimentally that the low-order components of the light field are rather constant over the scenes whereas high-order components are not. Using very simple models, we found a strong relationship between the low-order components and the geometrical layouts of the scenes.

OCIS codes: 120.5240, 150.2950.

1. Introduction

Photographers, painters, designers, and architects acknowledge that the quality of the light in scenes is one of the main determinants for the visual appearance of these scenes [1–4]. To make materials look convincing one should use "natural complex light fields" in the rendering process [5]. However, few studies [6,7] describe the fundamental regularities of natural light fields empirically. The meaning of the term "quality of light" and its properties in natural scenes remains unclear.

The purpose of our work is to investigate the optical properties of natural scenes. More specifically, our aim is to describe theoretically the quality of the illumination, which is a rather artistic concept, in terms of physical measures. Furthermore, we experimentally analyze the spatial properties of light fields within natural scenes. There is no common language to describe the quality of light and its effect on the appearance of an object. Different approaches are used in different fields depending on the goals. For instance, lighting engineers and designers adopt an integral approach using a wide range of parameters (luminance levels, diffuseness, uniformity, glare index, and many others). On the other hand, in computer graphics, the illumination is frequently simplified as much as possible; in most cases the combination of ambient and direct components does the trick. A similar approach is adopted in photographers' studios and "movie shooting stages" where the combination of diffuse and direct light sources produces convincing results for most objects.

Light fields of natural scenes are highly complex, containing low and high frequencies. Due to interreflections within scenes the light comes from every direction and therefore in general the light field cannot be determined solely by primary light sources. However, despite the complexity of illumination, even with the naked eye it is often possible to distinguish some basic properties of light such as the over-

0003-6935/07/297308-09$15.00/0

all brightness, the primary illumination direction, and the diffuseness.

The first part of this paper is devoted to a theoretical analysis of second-order lighting. It is convenient to analyze the properties of light fields using spherical harmonics decomposition because this allows us to represent complex lighting as a combination of components of different orders. We investigate the qualitative properties of the first three components (monopole, dipole, and quadrupole) and describe their physical meanings through the development of a theoretical framework in which Gershun's classical work on the radiometric properties of the light field is related to, and extended by, these current techniques. We also develop a graphical representation of the low orders that gives a simple and intuitive description of the radiance distribution.

Another goal of our study is to investigate the dependency of the light field on the geometrical layout of the scenes. A particular question that we are addressing here is how much the illumination varies from location to location within a scene and how the different orders of the light field behave as a function of location within a scene. Taking into account that natural scenes usually have few primary light sources and that most materials scatter light in a diffuse way, we hypothesized that the low-order components of the illumination should be more or less constant within a scene and depend systematically on the geometrical layout of the scene. To test these hypotheses we empirically investigated the light fields of several scenes by measuring local light fields at several points on each scene using the panoramic image technique.

2. Previous Work

The light field is a function that describes the amount of light traveling in every direction through every point in space. The term "light field" and the first systematic theory on this subject were introduced by Gershun in a paper on the radiometric properties of light in 3D space [8].

At a typical point in a natural scene light comes from all directions simultaneously. Gershun's light field is essentially the radiance distribution over all space and all directions. For instance, for uniformly diffuse illumination, where the radiance is the same for all directions, the radiance distribution function at a point is a sphere. For a parallel beam of light the radiance distribution function degenerates into a single direction in the direction of the beam.

Gershun's primary goal was to describe the net transfer of radiant power through space. He defined the "radiant flux density" as the net flux that passes through any given surface element from either side. Gershun introduced the notion of "light vector" such that the component of the light vector in the direction of the surface normal represents the net flux density. The direction of the light vector can be found directly from the radiance as the average direction, weighted by radiance, over all directions. This concept allowed Gershun to describe the light field as a classical 3D vector field. Moon and Timoshenko, who translated his work, already mentioned that "the physically important quantity is actually the illumination, which is a function of five independent variables, not three." The light vector directly defines the transfer of radiant power but does not define the full radiant structure (i.e., the lighting condition). Two light vectors may be identical whereas the radiance functions that underlie them may be quite different. In our work we introduce the quadrupole or squash tensor of the light field, to complement the light vector so as to describe the radiance distribution function in more detail. This may be considered as a small step toward the development that Moon and Timoshenko were aiming for in their foreword: "Is it not possible that a more satisfactory theory of theory of the light field could be evolved by use of modern tensor methods in a five-dimensional manifold?"

Gershun's theory was further developed and broadened by Moon in his work on the photic field [9]. In different areas the concept of radiance distribution has different names: In computer vision it is known as the plenoptic function [10], in the realm of computer graphics it was introduced as the lumigraph [11] or light field [12] and became very popular in applications for image-based modeling and rendering. Since then, several techniques of parametrizing and capturing light fields have been developed.

The analysis of light field properties in natural scenes started with the statistical analysis of intensity distributions in conventional images of natural scenes [13,14]. Due to the limited field of view and low dynamic range of conventional images, that approach was limited. Later Dror adopted a similar approach to high dynamic range panoramic images of the scenes, so-called "illumination maps" (one of the ways of capturing the incoming light field at a point). He performed a statistical analysis on several illumination maps that were photographed in different scenes and found some regularities in the intensity distributions in those images. The scenes were independent of each other, which leaves unanswered the questions: Is there a relationship between the intensity distribution in illumination maps and the geometrical envelopes of the scenes or illumination conditions of the scenes? If there is a relationship, how much does the light field vary within a scene?

The spherical harmonics [15,16] representation of the light fields appeared to be useful in many applications ranging from computer graphics rendering techniques to recognition algorithms in computer vision. It was shown theoretically [17,18] for convex Lambertian objects that the light field can be successfully replaced by its second spherical harmonics approximation without changing the objects' appearance much.

3. Theory

In this section we look into the low-order properties of lighting. When spherical harmonics decomposition is applied the radiance distribution function at a point can be represented as a sum of its frequency compo-

nents. We give a qualitative, physical description of the components up to the second order in terms of spherical harmonics. We show that the second-order component, the quadrupole or squash tensor, represents specific cases of lighting such as a "clamp" and a "ring" of light.

A. Spherical Harmonics Definitions

To describe the structure of light fields we utilize real spherical harmonics decomposition [15]. Any spherical function $f(\vartheta, \varphi)$ can be represented as the sum of its harmonics:

$$f(\vartheta, \varphi) = \sum_{l=0}^{\infty} \sum_{m=-l}^{l} f_{lm} Y_{lm}(\vartheta, \varphi), \tag{1}$$

the basis functions being defined as

$$Y_{lm}(\vartheta, \varphi) = K_{lm} e^{im\varphi} P_{lm}(\cos \vartheta), \quad l \in N, -l \le m \le l, \tag{2}$$

where P_{lm} are the associated Legendre polynomials and K_{lm} are the normalization constants:

$$K_{lm} = \sqrt{\frac{(2l+1)}{4\pi} \frac{(l-m)!}{(l+m)!}}, \tag{3}$$

and the real value basis is defined as

$$Y_{lm}(\vartheta, \varphi) = \begin{cases} \sqrt{2} K_{lm} \cos(m\varphi) P_{lm}(\cos \vartheta), & m > 0 \\ \sqrt{2} K_{l|m|} \sin(|m|\varphi) P_{l|m|}(\cos \vartheta), & m < 0. \\ K_{l0} P_{l0}(\cos \vartheta), & m = 0 \end{cases} \tag{4}$$

Spherical harmonics form an orthonormal basis on the unit sphere. Coefficients f_{lm} can be calculated as

$$f_{lm} = \int_{\varphi=0}^{2\pi} \int_{\vartheta=0}^{\pi} f(\vartheta, \varphi) Y_{lm}(\vartheta, \varphi) \sin(\vartheta) d\vartheta d\varphi. \tag{5}$$

The indices obey $l \ge 0$ and $-l \le m \le l$. Thus, order l consists of $2l + 1$ basis functions. Therefore the function can be represented as a sum of its components, i.e., different orders. Any order l can be represented as a vector of corresponding coefficients $SH_l(f) = \{f_{l-l}, f_{l-l+1}, \ldots, f_{ll}\}$ and the representation of the entire function is a combination of the orders, i.e., $SH(f) = \{SH_0(f), SH_1(f), SH_2(f), \ldots\}$.

The spherical harmonics representation depends on the orientation of the function, i.e., if R is an arbitrary rotation over S, then $SH(f) \neq SH(R(f))$ (see Fig. 1). Therefore, in general the vector of SH coefficients cannot be used as an unique descriptor of the 3D shape defined by that function. Although a rotation will change the coefficients, it does not change the energy of the orders. This property was used by

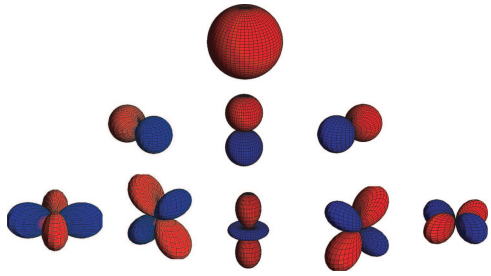

Fig. 1. (Color online) Spherical harmonics basis functions. The first row (the sphere) represents the zero order, the second row shows the basis functions of the dipole, the third row shows the basis functions of the quadrupole.

Kazhdan *et al.* [19] to construct rotationally invariant descriptors:

$$d_l = \sqrt{\sum_{m=-l}^{l} {f_{lm}}^2}. \tag{6}$$

Stock and Siegel [20] used a similar approach to characterize radiance distributions of different light sources. Physically, parameters d_l represent the power of the angular mode l. Siegel referred to d_l as the "strength of the angular mode l." The drawback of these coefficients is that they do not describe the function completely. For instance, if we rotated different components of a function arbitrarily and independently then the d_l profile of the resulting function would be the same, whereas the shape would be different. Therefore in general it is important to take into account the mutual orientation of different components as well as their strength.

B. Meaning of the Low-Order Components and Their Schematic Graphical Representation

For the zeroth- and first-order components the analogy between the spherical harmonics description and Gershun's theory is straightforward. The zero-order term, the monopole $\mathbf{M} = \{f_0\}$, corresponds to Gershun's "density of light," which is an integration of the radiance over the sphere. The monopole term is a fundamental property of the light field that describes the overall illumination at a point, i.e., how much radiance arrives at a point from all directions. From a computer graphics point of view the zero-order term can be thought of as an "ambient component."

The first-order term $\mathbf{D} = \{f_{1-1}, f_{10}, f_{11}\}$ can be thought of as a dipole, in view of the fact that in terms of spherical harmonics it consists of a positive and a negative mode. The orientation of the dipole corresponds to Gershun's light vector, the direction of maximum energy transfer at the point under consideration. The concept of the light vector allows us to represent light fields as vector fields.

The second-order term is the quadrupole $\mathbf{Q} = \{f_{2-2}, f_{2-1}, f_{20}, f_{21}, f_{22}\}$, which consists of five basis functions. The angular distribution according to a quadrupole is given by $Q(\vartheta, \varphi) = \sum_{m=-2}^{2} f_{2m} Y_{2m}(\vartheta, \varphi)$. Any order term with $l \ge 1$ consists of positive and

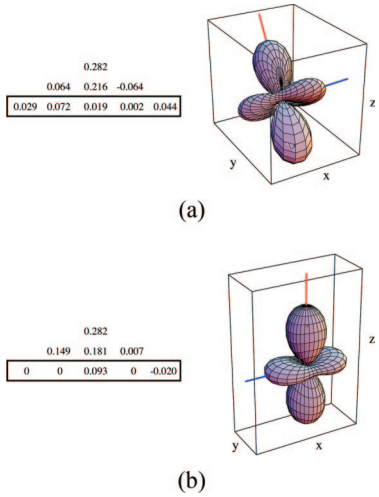

Fig. 2. (Color online) Second-order representation of a light field in the (a) original arbitrary orientation and (b) orientation with regard to the quadrupole. On the left side the first nine coefficients are presented (note the change after rotation); on the right side the quadrupoles are presented graphically. Note that the shape of the quadrupole does not change after rotation whereas the mathematical description is simplified and depends only on two coefficients $q^+ = 0.093$ and $q^- = -0.020$. The coefficients that make up the quadrupole are framed.

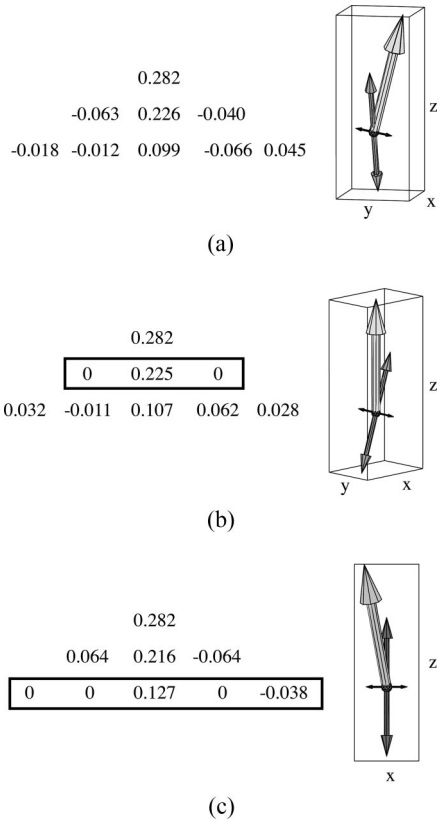

Fig. 3. Schematics of the second-order light field in (a) original orientation and (b) orientation aligned according to the light vector (c) orientation aligned according to the quadrupole. The *SH* coefficients are presented on the left side. The mutual orientation of the components D, q^+, and q^- is shown on the right side. The length of the light gray arrow corresponds to the value d_1 (strength of the light vector), the lengths of the dark gray and black arrows correspond to values q^+ and q^-.

negative components, and in the case of the quadrupole these components are orthogonal to each other. The orientation of the components can be found from the maximum (minimum) of $Q(\vartheta, \varphi)$. When proper rotation is applied any quadrupole can be represented as $\mathbf{Q}^{rot} = \{0, 0, q^+, 0, q^-\}$ by aligning the axes of the quadrupole along the coordinate axes, the positive component along Z and the negative along Y (see Fig. 2). This rotation provides the simplest representation of the quadrupole—just two parameters q^+ and q^- are enough to describe its shape (in other words: the quality).

Thus, the second-order approximation of the radiance distribution function can be determined by a small set of meaningful parameters: the density of light d_0; the direction of the light vector (ϑ_D, φ_D) and its strength d_1; the orientations of the quadrupole's axes $(\vartheta_{Q+}, \varphi_{Q+})$ and $(\vartheta_{Q-}, \varphi_{Q-})$ and parameters q^+ and q^-. See Fig. 3(a) for a schematic in which the arrows indicate the orientations of the light vector and axes of the quadrupole, and the lengths of the arrows are proportional to their strength: the values of d_1, q^+, q^-. This graphic representation together with the value d_0 completely determines the second-order lighting. Parameters d_0, d_1, d_2, q^+, and q^- can be used as a rotationally independent characterization of the light field.

The second-order representation can be further simplified by rotating the function in such a way that the components are aligned according to the coordinate's frame. Since the dipole is the strongest component in most cases (except for the monopole, which does not have an orientation), it might be more convenient to orient the light field according to the dipole such that the light vector is parallel to Z. Then the second-order representation of the light field will be $SH_2{}^D(LF) = \{\mathbf{M}^D, \mathbf{D}^D, \mathbf{Q}^D\} = \{\{d_0\}, \{0, d_1, 0\}, \{f_{2-1}{}^D, f_{2-1}{}^D, f_{20}{}^D, f_{21}{}^D, f_{22}{}^D\}\}$ [see Fig. 3(b)]. A rotation does not change the structure of the radiance distribution function, but it changes its orientation in global coordinates. The mutual orientation of the dipole and quadrupole remains the same under rotation. Because the light vector is fixed, the second-order description will now consist of eight parameters: d_0, d_1, ϑ_{Q^+}, φ_{Q^+}, ϑ_{Q^-}, φ_{Q^-}, q^+, and q^-.

In a similar way we can rotate the function in such a way that the axes of the quadrupole, which are orthogonal to each other, are oriented according to the coordinate axes Z and Y [see Fig. 3(c)]. Then the second order lighting is given by

$$SH_2{}^Q(LF) = \{\mathbf{M}^Q, \mathbf{D}^Q, \mathbf{Q}^Q\} = \{\{d_0\}, \{f_{1-1}{}^Q, f_{10}{}^Q, f_{11}{}^Q\}, \{0, 0, q^+, 0, q^-\}\}. \quad (7)$$

So here the structure of a second-order light field, which is independent of orientation, is given by six parameters: d_0, d_1, ϑ_D, φ_D, q^+, and q^-.

In all three cases [Figs. 3(a), 3(b), and 3(c)] the structure of the light field is the same. The rotation changes only its orientation in the global coordinate frame, whereas the mutual orientation of the components, their quality, and strength are the same. The representation in Fig. 3(a), shows that the original orientation of a light field in the global coordinate frame is useful when, for instance, we want to couple the radiance distribution function to the scene geometry. On the other hand, if we are interested only in the structure of the light field then representation (7) is more convenient because it restricts the coordinate frame and consists of fewer parameters.

The qualitative properties of the quadrupole are described in Subsection 3.C.

C. Qualitative Properties of the Quadrupole

The quadrupole has two components, one positive and one negative, that are orthogonal to each other and symmetric around the intersection point. As was shown in the previous section, the structure (quality) of a quadrupole can be described completely by two scalar parameters q^+ and q^-. Therefore keeping the strength of the quadrupole constant (d_2 constant) and varying q^+ and q^- such that $\sqrt{(q^+)^2 + (q^-)^2} = d_2$, we can achieve all possible structures of the quadrupole. The most extreme cases of light fields due to a quadrupole alone (light vector is assumed to be zero, the monopole component chosen is as small as possible such that the resulting function is nonnegative) appear to be a light clamp $q^+ = 1$, $q^- = 0$, and a light ring $q^+ = 0.5$, $q^- = \sqrt{3}/2$; see Fig. 4.

Figure 4(a) physically corresponds to two equal diffuse light sources positioned opposite to each other; we call this a "light clamp." Figure 4(b) corresponds to a diffuse "ring light source." Roughly speaking, from the coefficients q^+ and q^- we can assess how close the quadrupole is to one of those extreme cases.

By adding a light vector and changing the strengths and mutual orientations of the three components we can achieve a wide range of topologically different light fields.

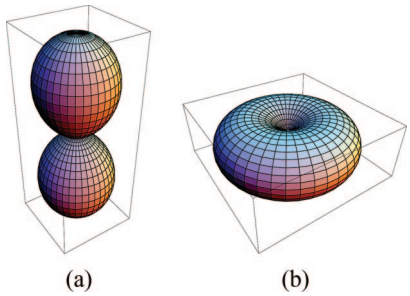

Fig. 4. (Color online) Qualitative properties of the quadrupole. Extreme cases of light fields due to the quadrupole: (a) light clamp, $q^+ = 1, q^- = 0$, (b) light ring, $q^+ = 0.5, q^- = \sqrt{3}/2$. The light vector is assumed to be zero, the monopole d_0 is chosen as small as possible such that the resulting function is nonnegative everywhere.

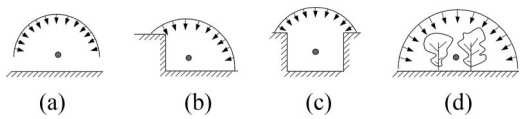

Fig. 5. Geometrical layouts of the measured scenes (a) open field, (b) wall, (c) street, and (d) forest.

D. Models for Simple Geometries: Street, Wall, Forest Scenes

To provide a more intuitive explanation of the light vector and quadrupole we will consider some very simple models of the light fields in several basic geometries. The geometrical layouts of the scenes are depicted schematically in Fig. 5.

The model of the open field scene consists of a uniformly bright sky (upper hemisphere) and uniformly bright ground (lower hemisphere) that is darker than the sky. The second-order representation of a light field in such a scene will contain only the light vector and the monopole. The quadrupole vanishes due to the symmetry of the brightness distribution function in the scene (in fact, all even components vanish). The light vector is oriented vertically to the middle of the sky opening and in this case indicates the symmetry of the light field. Due to the nonuniformity of materials and geometry in natural scenes (the sky is not uniformly bright, the ground is not Lambertian, the geometrical layout is not symmetrical), the brightness distribution function cannot be absolutely symmetrical; therefore in natural scenes the quadrupole generally does not vanish completely. However, in the scenes that are close to our assumptions (heavily overcast sky, uniform ground close to Lambertian, open space up to horizon) the quadrupole should become negligibly small in comparison with the light vector.

Figure 6(a) shows the model of the light field across a street scene. Again, the sky is assumed to be uniformly bright, the ground and the walls are uniform and Lambertian (the ground is brighter than the walls); interreflections were not taken into account.

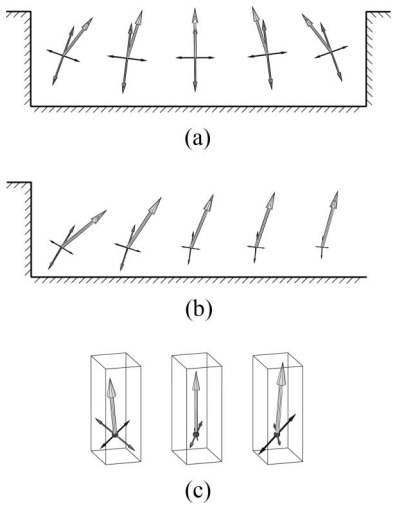

Fig. 6. Simplest models of the light field in the following geometries (a) street scene, (b) wall scene, and (c) forest scene.

We calculated the local light fields in five points across the scene. The light vector tends to be oriented approximately in the direction of the middle of the sky opening (direction of maximum energy transfer) and its orientation changes gradually from location to location; $\mathbf{q}^+$ is oriented primarily vertically according to the clamp composed of the brightest areas in the scene: sky and ground; $\mathbf{q}^-$ is oriented according to the darkest areas in the scene (walls), which can be thought of as a negative clamp. Note that the orientation of light field components changes smoothly as the geometrical layout changes.

Figure 6(b) depicts the wall scene, which is essentially the same as the street scene, but without one wall. Note that the strength of the quadrupole decreases as the distance to the wall increases and the closer the situation gets to the open field scene.

To investigate a scene in which the geometry varies more stochastically than in manmade scenes, we considered a forest scene. The illumination in a forest is due to the light scattering through the foliage and the gaps in the foliage. The upper hemisphere of the scene was modeled as a random distribution of 30° patches, each of different brightness. The lower hemisphere was modeled in the same way but the mean brightness value was lowered. We calculated the local light fields at three points in this scene. The results are shown in Fig. 6(c); the orientation of the light vector is vertical and varies a little from location to location, whereas the orientation of the quadrupole is random.

It was not our purpose to develop sophisticated detailed models of natural scenes; on the contrary, we tried to simplify them as much as possible. However, as it will be shown in Section 4, the light fields of corresponding real natural scenes show similar patterns to those of our much oversimplified models.

4. Empirical Studies

In the empirical study we considered three types of scenes, namely, a city street, a forest, and a wall (see Fig. 5). These scenes were chosen because they are common, simple (also to model), and possess different properties: the street and wall scenes have very distinct geometries; the geometry of the forest scene, on the other hand, is rather stochastic and does not have a clear envelope. Each type of scene was measured under two types of natural daylight illumination conditions: clear sky (close to collimated) and overcast sky (rather diffuse).

A. Data Acquisition

To estimate how the light field changes within each scene, we took three samples per scene at different locations. The samples were taken along a straight line, approximately 10 m apart and at a height of 1.5 m. The orientation of the line, along which the measurements were taken, was chosen in such a way that the geometrical layout of a scene remained approximately the same as viewed from the measurement locations. In the case of the city-street scene, the measurements were taken along the street; for the forest the direction of measurements was not important due to the isotropic character of the geometry of that scene (though of course it was kept constant with relation to the primary illumination). The wall scene was measured in two directions: along the wall, such that the geometry remained the same, and across the scene, orthogonally to the wall such that the geometrical layout varied systematically with distance.

At every point the local light field was measured as an illumination map: a high dynamic range panoramic image covering a whole sphere. To produce the panoramic image we used an Olympus E-20 digital camera with a fish-eye lens, attached to a rotation frame and mounted on a leveled tripod. We used a fish-eye lens with a 124° horizontal field of view. Each panorama consisted of 14 images made in different directions (the pictures overlapped by 30% to achieve a better result). To increase the dynamic range, the pictures were taken with three different exposure values. The pixel-by-pixel correspondence between the pictures of different exposures was achieved by using remote control and by making the pictures in the automatic bracketing mode.

The whole procedure of taking the pictures for three panoramas (126 pictures) took approximately 40 min. We decided to make measurements at approximately noon, so that the Sun did not move much during measurements and therefore illumination was relatively constant.

B. Data Processing

The images were corrected for radial brightness falloff and stitched together in a rectangular panoramic image. For this purpose we used commercially available software (PTMAC 3.00). The stitching procedure was applied separately for different exposures and three resulting panoramas were combined together into one high dynamic range illumination map according to the radiance response curve of the camera. The response curve was estimated using a technique described by Debevec and Malik [21]. The high dynamic range pictures were stored as arrays of floating-point values. The resolution was downsampled to 250×500.

5. Results

The panoramic images of the scenes considered are shown in Fig. 7 in a light probe format [22] (angular map). For each image we calculated spherical harmonics coefficients up to the sixth order. To the right of the panoramic images we depicted the cross sections through the SH_6 approximations of the corresponding local light fields, the directions of the cross sections being indicated by black circles in the panoramic images. The panoramic images show the actual scenes, whereas the cross sections give an impression of how the sixth-order approximation of a light field varies within scenes. For instance, in the panoramic images of the street scene under a clear sky illumination condition [Fig. 7(a)] there are two bright areas due to the Sun (top right; note: the Sun

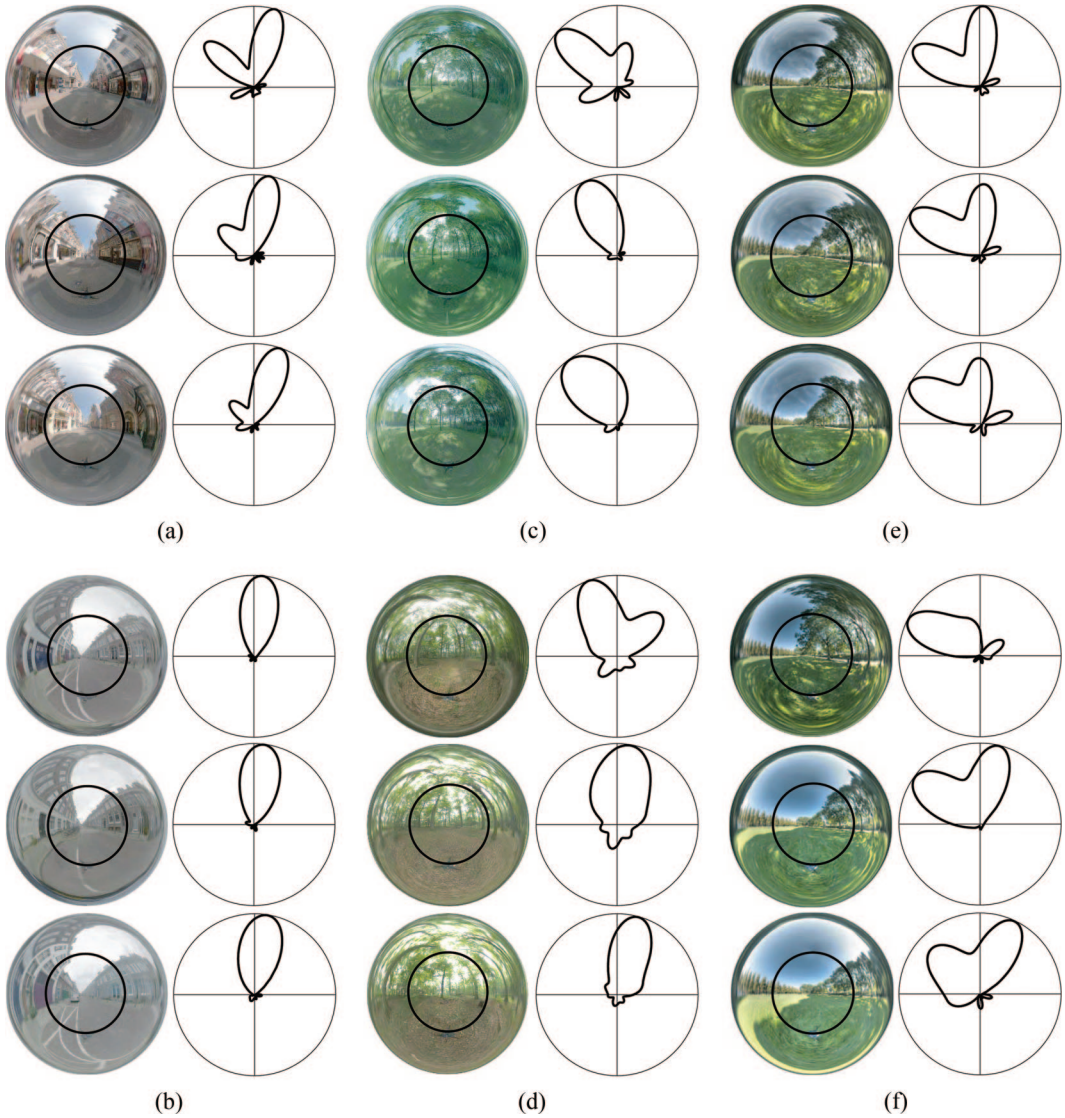

Fig. 7. (Color online) Light probes of (a) street scene under a clear sky, (b) street scene under an overcast sky, (c) forest under clear sky, (d) forest under an overcast sky, (e) "wall" scene measured along the wall, and (f) wall measured across. To the right of the panoramic images the cross sections through the SH_6 approximations of the corresponding local light fields are depicted; the directions of the cross sections are indicated by black circles in the panoramic images.

itself is not present in either of the panoramas) and due to strong scattering from the building on the left side of the street. These two brightest areas are distinguishable in the cross sections as modes in the corresponding directions. Note that the mode that corresponds to the bright sky area is stronger and the same in all three locations, whereas the second mode is hardly distinguishable in the third location (this is because the cross-section line runs through the relatively dark spot on the left building).

A similar situation exists in the "wall along" scene [Fig. 7(e)] in which one mode is due to the large opening in the sky on the left side of panoramas, and the second one is due to a bright halo around the Sun (the Sun is hidden behind the trees). Note how similar the profiles are for all three locations of this scene. In the "wall across" scene the geometrical layout of the scene varies from location to location and you can see [Fig. 7(f)] how the cross sections of the light fields transform from one mode at the first location into two modes at the third location.

In the forest scenes [Figs. 7(c), 7(d)] the primary sources of light are patches of open sky from the gaps in the foliage that are distributed rather stochastically over the upper hemisphere [23]. Therefore the radiance distribution function varies considerably. However, from the cross sections we can see that for each location there is only one strong mode that is oriented approximately vertically (light comes from above) but is slanted slightly in the direction of the largest opening in the foliage.

Note that because the panoramic images were photographed in equal orientations at all three measurement points of each scene, we can use the spherical harmonics coefficients and the cross-section profiles (which are calculated from spherical harmonics coef-

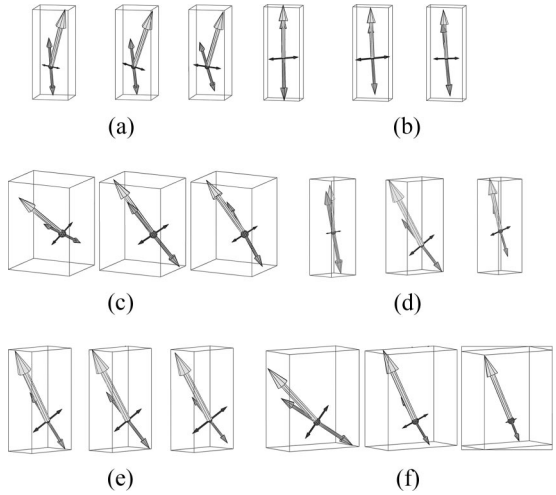

Fig. 8. Schematic of the second-order approximations of the local light field measurements. The letters represent the same scenes as in Fig. 7. For each scene figures that run from left to right correspond to the figures that run from top to bottom in Fig. 7.

ficients) to compare the local light fields straightaway without having to calculate the rotationally independent parameters.

Figure 8 shows the schematic of the second-order approximation of the samples. As explained in Section 3, this kind of representation gives the complete description of the second-order approximation of the local light fields. Comparing different samples you can see how the light vector changes its orientation and magnitude, how the quality and orientation of the quadrupole change from point to point. This kind of representation enables us to judge qualitatively the behavior of the low-order components of the light fields. The spherical harmonics coefficients for each sample were normalized by the zero-order component in order to give equal footing comparisons (here we

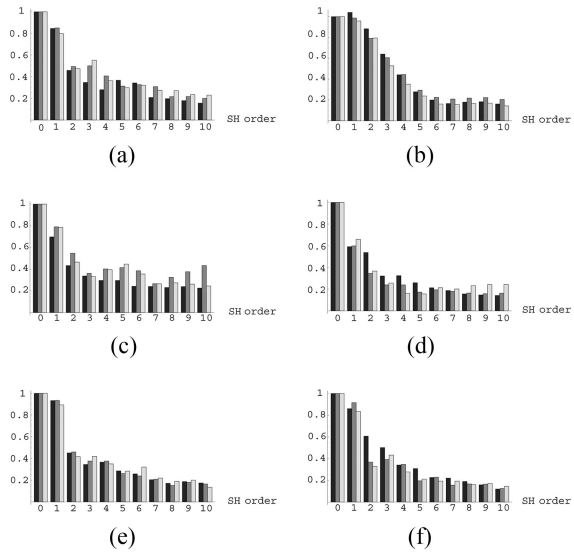

Fig. 9. Strengths d_1 of the light field components up to tenth order. The letters represent the same scenes as in Fig. 7; the bars of different gray levels represent three samples within the scene.

are mainly interested in the structure of light fields, not in the absolute values).

In Fig. 9 we depict the strengths of the different orders, i.e., coefficients d_l up to the tenth order. The parameter d_0 is equal to 1 for all samples in all scenes, because the spherical harmonics coefficients were normalized by the zero-order component. Coefficients d_l provide rotationally independent descriptors and physically represent the power of the corresponding angular mode l. Note that strengths of low orders are higher than those of high orders. Starting from the fourth to fifth order the d_l values fade away and level off at a value that is significantly smaller (approximately five times smaller) than the strengths of low orders.

6. Conclusion and Discussion

From Figs. 7 and 8 we can conclude that in the case of overcast diffuse illumination the light field varies less than in the case of clear sky. That is easy to explain from the properties of the scenes considered. As we can see from the panoramic images, in the street scenes the primary illuminations and geometrical layouts of the scenes are reasonably constant in the locations where the samples were made. Light field variation is mainly due to the secondary light sources, which vary within a scene due to the variation of the reflectance properties of materials that make up the scene, from location to location in that scene. The effect of these secondary light sources is much stronger in collimated illumination (clear sky) than in diffuse lighting (overcast sky) due to the directedness of the primary illumination. In the case of forest scenes, the light field variation is due to two factors, the geometrical layout of the scenes varies (the gaps in the foliage are stochastic) and secondary light sources are more significant in the case of clear sky illumination (note bright patches on the ground in the scene "c").

From Figs. 7 and 8 we can also say that the low-order components of the light field are more constant within a scene than are the high orders. Note in Fig. 8 that as long as the geometry of a scene remains reasonably constant, the low orders are very similar in different locations. However, if the position with regard to the geometry varies systematically, the low-order components vary systematically as well. The simple model of the wall scene [Fig. 6(b)] corresponds well to real measurements [Fig. 8(f)]; notice a similar tendency in component orientations and observe how the quadrupole decreases as the distance to the wall increases.

Figure 9 shows that the low-order components of the light fields within the scenes considered are the strongest. Low-order components define the main shape of the light field, whereas the higher orders have a more stochastic nature. We believe this fact can be used in modeling, the main properties of the light field (shape of the radiance distribution function) can be defined by low orders (density of light, light vector, quadrupole), whereas the high orders can be taken as stochastic values that do not change

the main properties of the light field, but add naturalness to it.

This work was supported by the Netherlands Organisation for Scientific Research (NWO).

References

1. A. Adams, *The Negative* (Little, Brown and Co., 1981).
2. T. S. Jacobs, *Drawing with an Open Mind* (Watson-Guptill, 1991).
3. L. Michel, *Light: the Space of Shape* (Wiley, 1995).
4. M. Baxandall, *Shadows and Enlightenment* (Yale U. Press, 1995).
5. R. W. Fleming, R. O. Dror, and E. H. Adelson, "Real-world illumination and the perception of surface reflectance properties," J. Vision **3,** 347–368 (2003).
6. R. O. Dror, T. K. Leung, E. H. Adelson, and A. S. Willsky, "Statistics of real-world illumination," in *Proceedings of the IEEE Computer Society Conference on Computer Vision and Pattern Recognition* (IEEE, 2001), pp. 164–171.
7. R. O. Dror, A. S. Willsky, and E. H. Adelson, "Statistical characterization of real-world illumination," J. Vision **4,** 821–837 (2004).
8. A. Gershun, "The light field," J. Math. Phys. **18,** 51151 (1939) (translated by P. Moon and G. Timoshenko).
9. P. Moon and D. E. Spencer, *The Photic Field* (MIT Press, 1981).
10. E. H. Adelson and J. Bergen, "The plenoptic function and the elements of early vision," in *Computational Models of Visual Processing,* M. Landy and J. Movshon, eds. (MIT Press, 1991), pp. 3–20.
11. S. J. Gortler, R. Grzeszczuk, R. Szeliski, and M. F. Cohen, "The lumigraph," in *Computer Graphics, Proc. SIGGRAPH96* (1996), pp. 43–54.
12. M. Levoy and P. Hanrahan, "Light field rendering," in *Proc. SIGGRAPH 96* (1996), pp. 31–42.
13. J. Huang and D. Mumford, "Statistics of natural images and models," in *Computer Vision and Pattern Recognition* (IEEE, 1999), pp. 541–547.
14. S. Teller, M. Antone, M. Bosse, S. Coorg, M. Jethwa, and N. Master, "Calibrated, registered images of an extended urban area," in *Proc. IEEE Computer Vision and Pattern Recognition* (CVPR, 2001), pp. 93–107.
15. T. MacRobert, *Spherical Harmonics: An Elementary Treatise on Harmonic Functions, with Applications* (Dover, 1947).
16. J. Jacson, *Classical Electrodynamics* (Wiley, 1975).
17. R. Ramamoorthi and P. Hanrahan, "On the relationship between radiance and irradiance: determining the illumination from images of a convex Lambertian object," J. Opt. Soc. Am. A **18,** 2448–2459 (2001).
18. P. N. Belhumeur and D. J. Kriegman, "What is the set of images of an object under all possible illumination conditions?" Int. J. Comput. Vision **28,** 245–260 (1998).
19. M. Kazhdan, T. Funkhouser, and S. Rusinkiewicz, "Rotation invariant spherical harmonic representation of 3D shape descriptors," in *Eurographics Symposium on Geometry Processing,* L. Kobbelt, P. Schrder, and H. Hoppe, eds. (EG Digital Library, 2003).
20. R. D. Stock and M. W. Siegel, "Orientation invariant light source parameters," J. Opt. Eng. **35,** 2651–2660 (1996).
21. P. E. Debevec and J. Malik, "Recovering high dynamic range radiance maps from photographs," in *Proceedings of ACM SIGGRAPH* (1997), Annual Conference Series pp. 369–378, 1997.
22. http://www.debevec.org/Probes/.
23. J. A. Endler, "The color of light in forests and its implications," in *Ecological Monographs 63* (Ecological Society of America, 1993), pp. 1–27.